Design variable structure fuzzy control based on deep neural network model for servomechanism drive system

Mohamed A. Shamseldin[1], Abdel Halim M. Bassiuny[2], Abdel Ghany M. Abdel Ghany[3]
[1]Department of Mechanical Engineering, Faculty of Engineering, Future University in Egypt, Cairo, Egypt
[2]Department of Mechatronics Engineering, Faculty of Engineering, Heliopolis University, El Salam City, Egypt
[3]Department of Electrical Engineering, Higher Engineering Institute, Thebes Academy Cairo, Egypt

Article Info

Article history:

Received Dec 3, 2021
Revised Jul 18, 2022
Accepted Aug 1, 2022

Keywords:

Deep neural network
Fuzzy logic
Harmony research
Model reference
Servomechanism
Variable structure

ABSTRACT

This paper presents a new scheme for variable structure (VS) fuzzy PD controller. The rule base of the fuzzy PD controller is tuned online. The purpose of the proposed controller is to track accurately a preselected position command for the servomechanism system. Therefore, this study establishes a model using a black-box modeling approach; simulations were performed based on real-time data collected by LabVIEW and processed using MATLAB. The input signal for the servomechanism driver is a pseudo-random binary sequence that considers violent excitation in the frequency interval. The candidate models were obtained using linear least squares, nonlinear least squares, and deep neural network (DNN). The validation results proved that the identified model based on DNN has the smallest mean square errors. Then, the DNN identified model was used to design the proposed control techniques. A comparison had been executed between the VS fuzzy PD control, the conventional PD control, and the fixed structure fuzzy PD control. The experimental results confirm the proposed VS fuzzy PD control can absorb the nonlinear behavior of the system. The speed regulation test, it reduces the rise time from 50% to 56%. While continuously changing in speed, it has the smallest tracking error (0.412 inches).

Corresponding Author:

Mohamed A. Shamseldin
Department of Mechanical Engineering, Faculty of Engineering, Future University Egypt
End of 90th St. Fifth Settlement, New Cairo, Egypt
Email: Mohamed.abelbbar@fue.edu.eg

1. INTRODUCTION

The one-stage servomechanism system is the basic unit of most CNC machines [1]. These types of machines need accurate motion control to produce high-quality products [2], [3]. Also, the high speed and high accuracy position applications have been rapidly and broadly developed to facilitate the complex automatic processes in the industrial field [4], [5]. Generally, the servomechanism systems don't have an accurate estimated parameter for friction and backlash models which leads to system uncertainty. The friction causes high steady-state error while the backlash reasons undesired vibration in the system [4]. The models that can describe the friction phenomenon in servomechanism systems suffer from parameter uncertainty [6]. So, the control task for this operation faces a big challenge [7]. There are many design schemes for single-axis controllers such as conventional PID control, self-tuning proportional–integral–derivative (PID) control, fuzzy PID control, adaptive control, and sliding mode control [8]. The advantage of self-tuning and sliding mode techniques is that the tracking performance is good under the different operating points of position commands [9], [10]. In several applications, the sliding mode control has been applied such as microgripper position/force control as presented in [11] and the position control of X-Y stage servomechanism as demonstrated in [12].

On the other side, the disadvantages are that the chattering phenomenon can be an obstacle to improve the control accuracy, and in some cases, it causes instability in the system [13], [14]. The fuzzy logic system is a suitable technique to treat the uncertainty and nonlinear problems of complex systems [15], [16]. Sometimes, the fixed rule base structure of the fuzzy system cannot deal with system uncertainty and nonlinearity so, several previous studies had attempted to use different techniques to develop an adaptive mechanism that can tune online the rule base or normalizing gains as in [17], [18]. However, the disadvantage of these mechanisms takes a long time to adjust accurately the rule base and need high processing, so it cannot execute practically [19], [20].

It is known that the model reference adaptive control (MRAC) is highly efficient adaptive control mechanism where it forces the overall system to follow the behavior of a designed model reference [21]. The selected model reference can be a first or second-order system according to the point of view of the designer [22], [23]. Experimental identification is a well-recognized methodology to obtain a precise process model, often intended for control but also other purposes. The nature of the input signal for the identification has a great effect on the accuracy of the model. But, in many cases, the input signal cannot be easily selected concerning plant behavior constrictions. pseudo-random binary sequences (PRBS) are often used as violent excitation signals for system identification, due to it has a finite length and can be synthesized frequently with simple generators while presenting favorable spectra for identification [24].

The family of candidate models for system identification can be classified along with several different aspects. The linear and nonlinear theory has been well developed and investigated for real applications throughout recent years. The linear structure is used to simplify the analysis where the parameters are constant and do not vary throughout a simulation, such as the autoregressive with exogenous inputs (ARX) model. In contrast, a non-linear model presents dependent parameters that are permitted to vary throughout a simulation run, and its use becomes necessary where interdependencies between parameters cannot be considered insignificant [25].

Lately, deep learning has become attractive and has significant attention from a wide range of engineering applications. Compare to traditional neural networks, the vital features of deep learning are to have more hidden layers and neurons and to improve learning performance [26]. Using these features, complex and large problems that could not be solved with traditional neural networks can be resolved by deep learning algorithms [27]. Therefore, deep learning has been subjected to various applications including pattern recognition and classification problems; for example, handwritten digit recognition, speech recognition, human action recognition, and so on. However, to the best knowledge of the authors, no result has been published in the system identification and automatic control field [28]. Thus, this paper focuses on presenting the applying possibility of deep learning in system identification areas.

This study investigates the performance of a one-stage servomechanism system using several advanced control techniques. Firstly, identified models using linear least squares, nonlinear least squares, and DNN had obtained and selected the best between them. Both the conventional PD and fixed rule base fuzzy PD controller had investigated but still, the performance is not acceptable. Therefore, a new variable structure (VS) fuzzy PD controller had designed to tune the rule base online using an adaptive mechanism with fast calculation to can apply practically. The parameters of the adaptive mechanism had obtained based on the selected model reference. The optimal parameters of the proposed control techniques had been determined using harmony search (HS) optimization technique. The paper is prepared as follows, firstly, the experimental setup is presented. Secondly, system identification is explained. Thirdly, the proposed controller techniques are demonstrated. Fourthly, the experimental results are illustrated. Finally, the conclusion is discussed.

2. EXPERIMENTAL SETUP

This section demonstrates the main parts of the one-stage servomechanism system prototype. Also, it shows the open-loop performance of the servomechanism system. Figure 1 illustrates the main components of one stage servomechanism experimental setup which consists of a DC motor electro-mechanical module. The stroke of the stage ranges from 0 to 9 Inches.

The DC motor has a nominal speed of 1800 rev/min, and an armature voltage of 90 V dc. The optical encoder is an add-on that provides position feedback signal (200 pulses per revolution). Two magnetic limit switches detect when the sliding block reaches the start or end position. The DC motor drive controls the DC motor electro-mechanical module. This versatile drive also allows an external signal to control the motor speed. A data acquisition card (DAQ) NI USB-6009 is connected to the computer that is used to perform the control algorithms. The main idea of the program has been designed to make the NI

DAQ 6009 generates an analog output signal (-5 to 5 V) to the linear amplifier. Also, the analog output signal from the optical encoder has been collected at the same time. The speed of the DC motor will fluctuate when the generated signal change continuously. The positive signal will cause the DC motor speed to fluctuate in the forward direction, while the DC motor will fluctuate in the reverse direction through the negative voltage ranges. The shaft of the optical encoder is coupled with the lead screw shaft to measure the speed and position of the stage as in Figure 2.

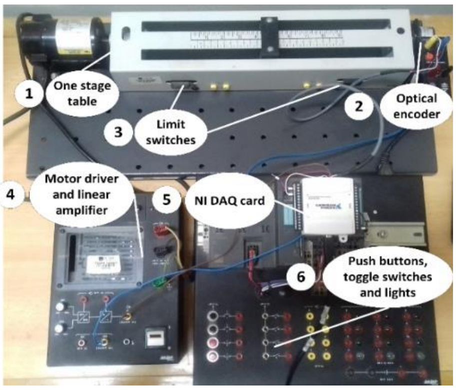

Figure 1. The one stage servomechanism experimental setup

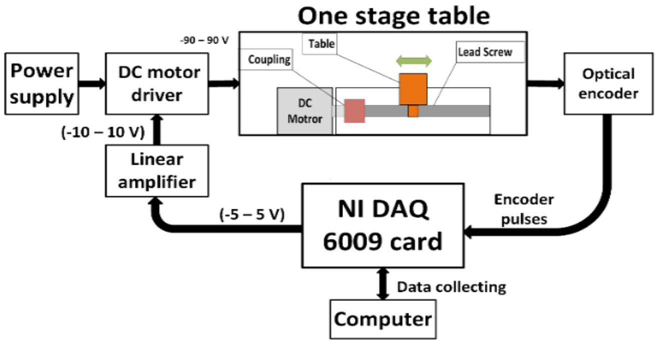

Figure 2. The block diagram of the experimental setup servomechanism system

Figure 3 demonstrates the PRBS output signal from the NI DAQ card. It can be noted that the signal has a variable frequency at an acceptable range. Then, this signal will be input to the DC motor driver. Figure 4 shows the corresponding linear speed of the stage measured by the optical encoder. It is clear that the linear speed was fluctuating highly due to the violent excitation of the servomechanism system. Therefore, the stage position increases in positive ranges of the input signal entering to DC motor driver while the actual stage position decreases in negative ranges of the input signal. The input/output data will be collected and stored in an excel sheet file and then this data will be used to develop an identified model for the experimental setup.

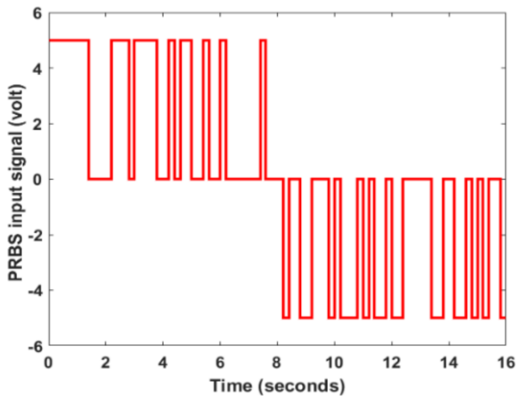

Figure 3. The random output signal of the NI DAQ card

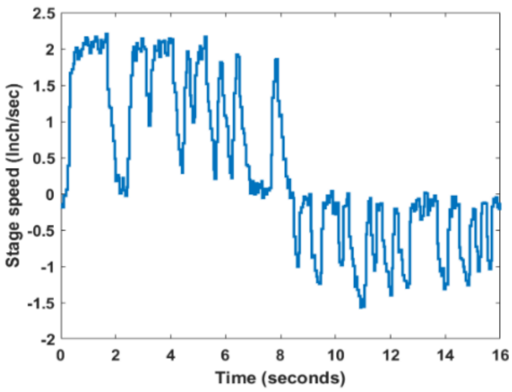

Figure 4. The output linear speed of the servomechanism table

3. SYSTEM IDENTIFICATION

This section investigates an accurate model for a one-stage servomechanism system based on measured input/output data. Three system identification techniques will be used. The first technique uses linear least squares. The second technique is the nonlinear least squares. Lastly, the third technique develops a DNN-identified model.

3.1. Linear least squares model

The general linear transfer function can be expressed as follows:

$$\frac{y(s)}{u(s)} = \frac{k}{b_n.S^n + b_{n-1}.S^{n-1} + \cdots + b_0} \quad (1)$$

In (1), $k, b_n, \ldots, b_0$ are the estimated parameters of the approximate transfer function (T.F). The y(s) stands for linear stage speed while u(s) is the input voltage to the DC motor drive. The accuracy of the transfer function improves significantly when the system degree is increased. However, often there is a restriction that increasing order cannot make the model accurate sufficiently [29]. Therefore, it is necessary to explicitly add the nonlinearities into the system [30].

3.2. Nonlinear least squares model

As the servomechanism systems suffer from uncertainty and complex nonlinear dynamics, a nonlinear ARX (NLARX) model structure has been developed to model such systems [31]. The NLARX model consists of several complicated nonlinear functions that can model the backlash and friction in servomechanism systems significantly. An NLARX model can be understood as an extension of a linear model. A linear SISO ARX model has this structure [32].

$$y(t) + a_1 y(t-1) + a_2 y(t-2) + \cdots + a_{na} y(t-na) = b_1 u(t) + b_2 u(t-1) + \cdots + b_{nb} u(t-nb+1) + e(t) \quad (2)$$

Where u is input, y is output, na is the number of past output terms and nb is the number of past input terms. This structure can be extended to create a nonlinear form where instead of the weighted sum that represents a linear mapping, the NLARX model has a more flexible nonlinear mapping function [33].

$$y(t) = f(y(t-1), y(t-2), y(t-3) \ldots., u(t), u(t-1), u(t-2), \ldots) \quad (3)$$

Where f is a nonlinear function (to simulate the behavior of friction and backlash that exist in servomechanism systems). Inputs to f are model regressors.

3.3. Deep neural network model

There are two main types of ANN, the first type is the shallow neural network and the second type is the deep neural network. Deep learning has several layers of hidden units and it also permits many more factors to be used before over-fitting occurs. Thus, for deep learning, a deep architecture is used. The neural network structure in this study contains three layers the first layer is the input layer which receives the input PRBS signal to the DC motor driver. The second layer is the hidden layer that contains several hidden neurons and receives data from the input layer. The third layer is the output layer which presents the corresponding linear stage speed. $x_i = (x_1, x_2, x_3, \ldots, x_n)^t$ Input vector applied to the layer, the whole of the hidden neuron input 'j' is:

$$net_j^h = \sum_{i=1}^{n} w_{ij} X_i + \theta_j^h \quad (4)$$

With $X_i = (X_1, X_2, X_3, \ldots, X_n)^t$ (5)

such as $i = 1,2, \ldots, N_h$

x_i is the input vector applied to the layer, and w_{ij} is the weights of (i) input neuron connection, and θ_j^h represent the bias of hidden layer neurons. The neurons of the hidden layer can be written as follows:

$$y_j^h = f\left(\sum_{i=1}^{n} w_{ij} X_i + \theta_j^h\right) \quad (6)$$

3.4. Candidate identified models validation

The obtained input/output data was used to develop a set of three candidate-identified models to select the best between them. Three models had been obtained, the first identified model is a linear second-order system while the second identified model is an NLARX model and lastly, the DNN identified model. The linear second-order system has the following specifications.

$$\frac{y(s)}{u(s)} = \frac{27.05}{s^2 + 13.91s + 78.45} \quad (7)$$

By matching with in (1), the estimated parameters of the linear approximation transfer function are $k = 27.05$, $n = 2, b_n = 1$, $b_{n-1} = 13.91$ and $b_0 = 78.45$. On the other hand, the obtained discrete-time ARX model has the following structure.

$$A(z)y(t) = B(z)u(t) + e(t) \tag{8}$$

Where:
$A(z) = 1 - 0.7564\, z^{-1} - 0.09098\, z^{-2}$
$B(z) = 0.03327\, z^{-1} + 0.01742\, z^{-2}$

By corresponding with in (2), the polynomial orders are $na = 2$ and $nb = 2$. Also, the used nonlinear function is a wave net with 25 units. Figure 5 demonstrates the linear speed of the actual experimental setup and the candidate models. It is noted that the identified model based on DNN can simulate the behavior of an actual experimental setup compared to other identified models. Table 1 demonstrates the mean square error of candidate models. It can be noted that the identified model based on DNN has a minimum error compared to other identified models.

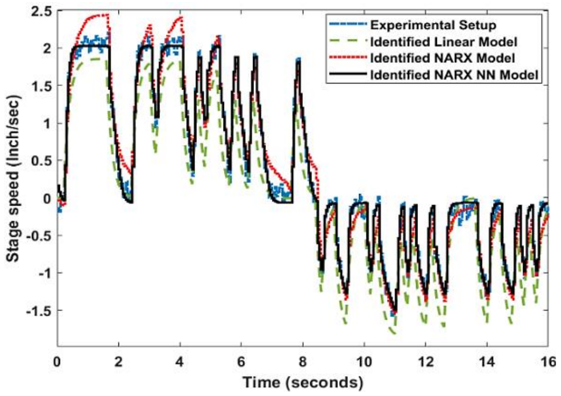

Figure 5. The linear speed of one stage table servomechanism for actual experimental setup and identified models

Table 1. Mean square error of candidate models

No.	System identification method	Mean square error
1	Identified Model (Second Order T.F.)	0.1973
2	Identified System (Nonlinear ARX model)	0.05912
3	Identified NARX neural network model	0.00071

4. VARIABLE STRUCTURE FUZZY PD CONTROL

4.1. VS fuzzy PD control

There are two types of adaptive fuzzy controllers. The first type tunes the rules of the fuzzy system so, it is called self-organizing controllers or variable structure controllers [34]. In the second type of fuzzy controller, the scaling factors are modified online and can be called self-tuning controllers [35]. The previous studies showed that the first type of adaptive fuzzy controller is more effective than the second type [36]. But, the first type of adaptive fuzzy controller is more complicated than the second type where the first type needs building the fuzzy system by the designer without using the fuzzy toolbox for any software program [37]. The proposed technique has an adaptive mechanism to tune the centroid of rule base membership online based on the optimal model reference adaptive system. Figure 6 illustrates the general structure of variable structure fuzzy PD control.

The variable structure fuzzy PD control input/output relationship can be described as follows:

$$u(s) = GU.\Delta u(s) \tag{9}$$

$$\Delta u(s) = \underline{\theta}^T \underline{z}(\underline{x}) \tag{10}$$

$$E(s) = GE.e \tag{11}$$

$$CE(s) = GCE.ce(s) \tag{12}$$

$$GE = 1,\ GCE = \frac{k_d}{k_p}, GU = k_p \tag{13}$$

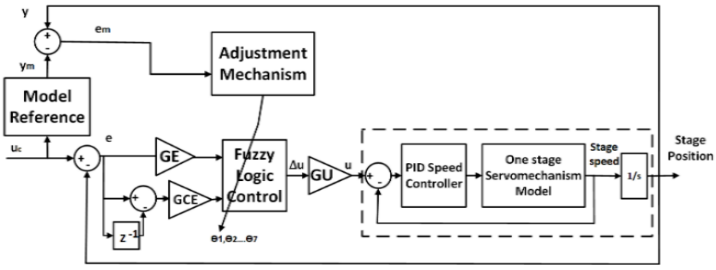

Figure 6. Variable structure fuzzy PD (VSFPD) control

Where $u(s)$ is the output fuzzy controller, where $\underline{\theta}^T$ is the centroid vector of the output membership function, $\underline{z}(\underline{x})$ is the vector of the fuzzy basis function, $x \in [-1,1]$, and GU is the scaling factor for the fuzzy PD controller. Inputs of the fuzzy controller are scaled using, GCE scaling factors also known as fuzzy gains, $e(s)$ is the error between the reference position and the actual position of the stage and $ce(s)$ is the change of this error as shown in Figure 7. Here, we introduce a reference model in the structure of the fuzzy controller to generate the model error given by:

$$e_m(s) = y(s) - y_m(s) \tag{14}$$

In (7), the $y(s)$ is the actual system output, the $y_m(s)$ stands for the desired performance and $e_m(s)$ considers the difference between the actual process value and the expected value of output. The reference model can be a first or second-order system. The model reference transfer function contains the desired response of the system such as the desired damping ratio, the desired natural frequency, the desired rise time, the desired settling time, and the desired overshoot. If the order of the reference model is a stable first-order system as the following transfer function.

$$\frac{y_m(s)}{u_c(s)} = \frac{k_m}{t_m s+1} \tag{15}$$

Where u_c is the reference position, y_m is the output of the reference model, k_m represents the DC gain of the system ratio between the input signal and the steady-state value of output and T_m is the time constant that measures how quickly a first-order system responds to a unit step input. The MIT rule is the original approach to MRAC. The name is derived from the fact that it was developed at the Instrumentation Laboratory (now the Draper Laboratory) at MIT. To adjust parameters in such a way that the loss function is minimized [38].

$$j(\underline{\theta}) = \frac{1}{2} e_m^2 \tag{16}$$

To make j small, it is reasonable to change the parameters in the direction of the negative gradient of j, that is,

$$\frac{d\boldsymbol{\theta}}{dt} = -\gamma \frac{\partial j}{\partial \underline{\boldsymbol{\theta}}} = -\gamma e_m \frac{\partial e_m}{\partial \underline{\boldsymbol{\theta}}} \tag{17}$$

where γ stands for the adaptation gain while $\underline{\theta}$ is the centroid vector of the output membership function. Figure 8 demonstrates the adaptive output membership functions for VSFC. The linguistic labels of the outputs are {NB(θ_1), NM(θ_2), NS(θ_3), ZE(θ_4), PS(θ_5), PM(θ_6), PB(θ_7)}. The output memberships centers are not fixed and change continuously through a certain range to prevent the overlapping between the memberships. Table 2 summarizes the adaptive rule base of VS fuzzy system.

From the adaptive output of the membership function can outcome the following equations.

$$\underline{\theta}(0) = [-1 - 0.66 - 0.33\ 0\ 0.33\ 0.66\ 1] \tag{18}$$

$$\underline{\theta} = [\theta_1\ \theta_2\ \theta_3\ \theta_4\ \theta_5\ \theta_6\ \theta_7] \tag{19}$$

The used defuzzification technique is the center of gravity.

$$u(nT) = \frac{\sum_{j=1}^{n} u(u_j)u_j}{\sum_{j=1}^{n} u(u_j)} = \underline{\theta}^T \underline{\mathfrak{z}}(\underline{x}) \tag{20}$$

Where $u\ (u_j)$ membership grad of the element u_j, $u(nT)$ is the fuzzy control output, n is the number of discrete values in the universe of discourse.

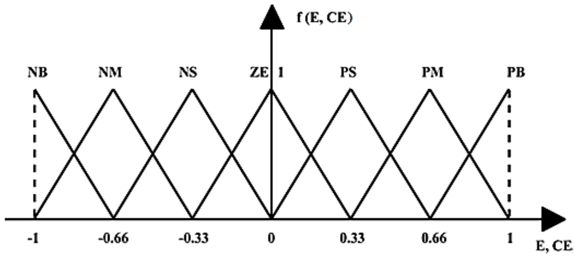

Figure 7. The input of membership functions (error and change of error)

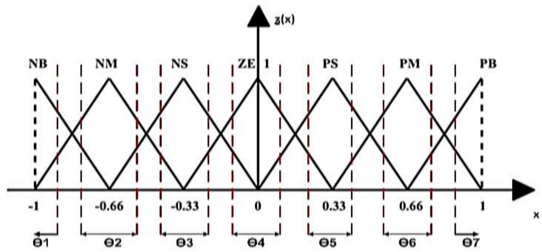

Figure 8. The adaptive output membership functions

Table 2. The adaptive fuzzy rule base

E/CE	NB	NM	NS	ZE	PS	PM	PB
NB	NB(θ_1)	NB(θ_1)	NB(θ_1)	NB(θ_1)	NM(θ_2)	NS(θ_3)	ZE(θ_4)
NM	NB(θ_1)	NB(θ_1)	NB(θ_1)	NM(θ_2)	NS(θ_3)	ZE(θ_4)	PS(θ_5)
NS	NB(θ_1)	NB(θ_1)	NM(θ_2)	NS(θ_3)	ZE(θ_4)	PS(θ_5)	PM(θ_6)
ZE	NB(θ_1)	NM(θ_2)	NS(θ_3)	ZE(θ_4)	PS(θ_5)	PM(θ_6)	PB(θ_7)
PS	NM(θ_2)	NS(θ_3)	ZE(θ_4)	PS(θ_5)	PM(θ_6)	PB(θ_7)	PB(θ_7)
PM	NS(θ_3)	ZE(θ_4)	PS(θ_5)	PM(θ_6)	PB(θ_7)	PB(θ_7)	PB(θ_7)
PB	ZE(θ_4)	PS(θ_5)	PM(θ_6)	PB(θ_7)	PB(θ_7)	PB(θ_7)	PB(θ_7)

4.2. Harmony search (HS) optimization

The HS is a phenomenon-mimicking algorithm inspired by the improvisation process of musicians [39]. Each controller variable corresponds to each musician [40]. The range of the parameter's value corresponds to the musical instrument's pitch range [41]. The solution matrix corresponds to the musical harmony at a certain time. In this paper, the HS optimization technique was used to obtain the optimal values of VS fuzzy PD controller based on MRAS ($\boldsymbol{\gamma}$ is the adaptation gain vector, k_m is the DC gain, T_m is the desired constant time and the scaling factors of the fuzzy system). The initial population of Harmony Memory (HM) is chosen randomly through a preselected range for each controller parameter. HM consists of harmony memory solution (HMS) matrix as in (21).

$$HM = \begin{bmatrix} GU_{(1,1)} & GE_{(1,2)} & GCE_{(1,3)} & \gamma_{1\,(1,4)} & \cdots & \gamma_{7\,(1,10)} & K_{m\,(1,11)} & T_{m\,(1,12)} \\ GU_{(2,1)} & GE_{(2,2)} & GCE_{(2,3)} & \gamma_{1\,(2,4)} & \cdots & \gamma_{7\,(2,10)} & K_{m\,(2,11)} & T_{m\,(2,12)} \\ \vdots & \vdots & \vdots & \vdots & \vdots & \vdots & \vdots & \vdots \\ GU_{(HMS,1)} & GE_{(HMS,2)} & GCE_{(HMS,3)} & \gamma_{1\,(HMS,4)} & \cdots & \gamma_{7\,(HMS,10)} & K_{m\,(HMS,11)} & T_{m\,(HMS,12)} \end{bmatrix} \tag{21}$$

Similarly, the HM matrix has been established for other proposed controller parameters (classical PD control and fixed structure fuzzy control). The objective function corresponds to the audience's aesthetics to be minimized or maximized. The used objective function is shown in (22).

$$f = \frac{1}{(1-e^{-\beta})(M_p + e_{ss}) + e^{-\beta}(t_s - t_r)} \tag{22}$$

Where M_p is the overshoot of system response, e_{ss} is the steady-state error, t_s is the settling time and t_r is the rise time. Also, this objective function can compromise the designer demand by the weighting parameter value (β). The parameter is set larger than 0.7 to reduce overshoot and steady-state error. If this parameter is set smaller than 0.7 the rise time and settling time will be reduced.

The HS optimization program contains several steps. The first step, initialize the HS parameters. In the second step, generate random values for the HM matrix and determine the fitness function corresponding to each solution vector. The third step, Improvise a new harmony from the HM matrix. The fourth step, replace the worst solutions with the best solutions. In the fifth step, repeat step 2 and step 4 until the termination criterion is satisfied. Table 3 demonstrates the obtained parameter values using HS optimization for the proposed controllers.

Table 3. The parameter values of the proposed controllers

Controller	Parameter	Value
PD controller	k_p	26.1677
	k_d	1.7924
Fuzzy PD controller	GE	0.087
	GCE	0.0456
	GU	3.01
VS Fuzzy PD controller	k_m	1.01
	T_m	0.102
	GE	0.092734
	GCE	0.00054574
	GU	40
	γ_1	0.04
	γ_2	0.045
	γ_3	0.056
	γ_4	0.078
	γ_5	0.089
	γ_6	0.0233
	γ_7	0.0123

5. EXPERIMENTAL RESULTS

This section demonstrates the motion behavior of one stage servomechanism system using the variable structure fuzzy PD control. Also, the performance of the proposed controller technique had been investigated by comparing it with the PD control and the fixed structure fuzzy PD control. Two tests had been applied to the experimental setup. In the first test, the position command was adjusted at a constant value while the second test was executed at the variable position command.

5.1. Constant position command

In this test, the position command was adjusted at a constant value (7 inches) and the stage began its motion from the position reference (zero inches). Figure 9 shows the position responses of the stage using three various control techniques. It can be noted that the variable structure fuzzy PD control has a minimum rise time and minimum settling time compared to other control techniques. Also, the variable structure fuzzy PD control has no overshoot approximately as demonstrated in Table 4.

Figure 10 demonstrates the corresponding linear speed responses of the stage through the experiment. It can be obvious that the variable structure fuzzy PD control has a high speed at the rise time. Also, it is decaying rapidly at moment 2 seconds to compensate for the error in the stage position. Then, the stage speed stables at zero approximately.

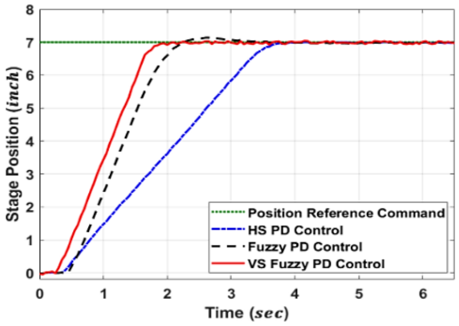

Figure 9. The stage position responses of proposed controllers at constant position command

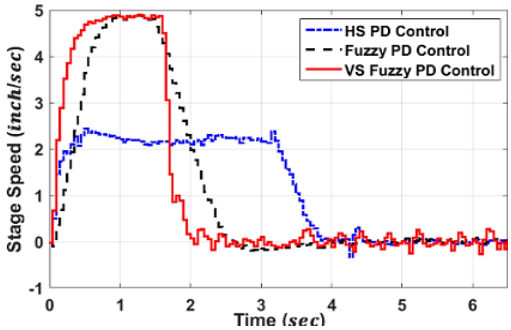

Figure 10. The stage speed responses of proposed controllers at constant position command

Figure 11 demonstrates the proposed controller's output through the experiment. The output signal in the case of the VS fuzzy PD control referred to the output after the gain GU. It is clear that all controllers give the maximum value at the beginning of the test which makes the stage accelerate rapidly to reach the desired position. Figure 12 illustrates the online change in the output membership centers through the constant position command test. It is noted that the adaptive mechanism tunes ($\theta 1$, $\theta 2$, $\theta 3$, and $\theta 4$) where the fuzzy output value locates through these memberships so, the other membership centers ($\theta 5$, $\theta 6$, and $\theta 7$) are not changed.

Table 4. The performance at constant position command test

Controller type	Rise time (sec)	Settling time (sec)	Overshoot (%)
The HS PD control	2.7123	3.5678	0.2123
The fuzzy PD control	1.6512	2.6565	2.0702
The VS fuzzy PD control	1.2344	1.8343	0.1778

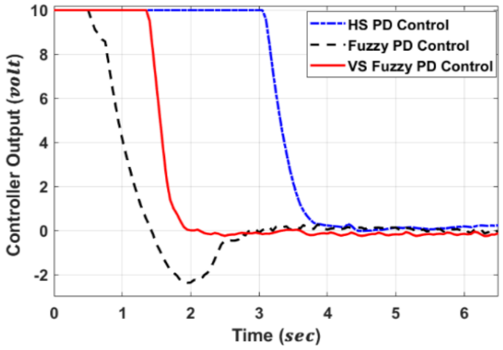

Figure 11. The stage position responses of proposed controllers at constant position command

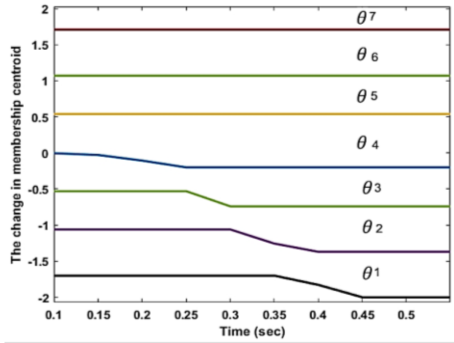

Figure 12. The change in membership centers during the constant position command test

5.2. Variable position command

The position command in this test changes continuously to investigate the robustness of the proposed controller technique and its ability to track a complex position command profile. Figure 13 illustrates the position responses of the stage by several control techniques and under variable position command (half-sine wave). It is obvious that the variable structure fuzzy PD control can follow accurately the complicated trajectory compared to other control techniques. Also, the fixed structure fuzzy PD control has acceptable tracking accuracy but it has a high error at the beginning of tracking while the harmony search (HS) PD control has a high deviation from the position command profile. Moreover, the variable structure fuzzy PD control has the smallest mean square error throughout the experiment as demonstrated in Table 5. Figure 14 demonstrates the corresponding linear speed responses of the stage for control techniques. It can be noted that the stage speed through the variable structure fuzzy PD control has a high value in the first seconds of the experiment and then the stage speed decreases gradually to track the position command profile.

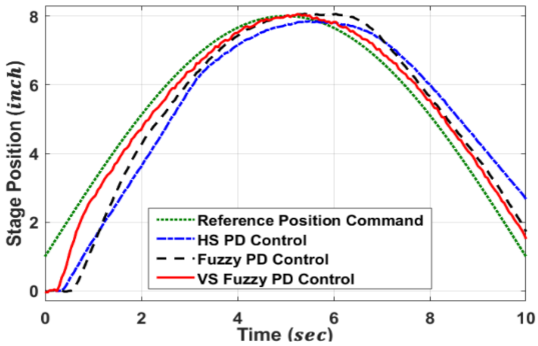

Figure. 13. The stage position responses of each control technique at variable

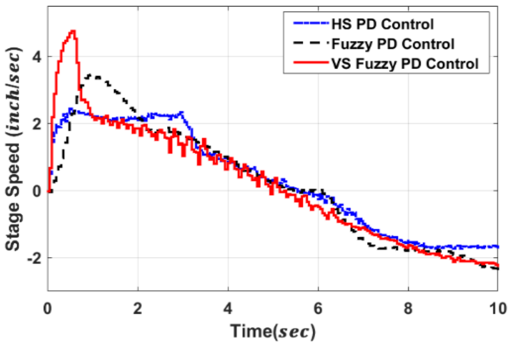

Figure 14. The stage speed responses of control techniques at variable position command

Table 5. The mean square error of proposed controllers at variable position reference command

Controller Type	Mean square error (inch)
The PD control	0.912
The fuzzy PD control	0.7065
The VS fuzzy PD control	0.412

Figure 15 shows the controller's output through the variable position command test. At the start of the experiment, the controllers have a high output value. These signals decrease gradually with different behaviors. The controller's signal declines until the polarity of signals change which leads to the reverse of the stage motion direction. Figure 16 shows the online change in the output membership centers during the variable position command test. It is obvious that the adaptive mechanism changes ($\theta 1$, $\theta 2$, $\theta 3$, and $\theta 4$) where the fuzzy output value belongs to these memberships so, the other membership centers ($\theta 5$, $\theta 6$, and $\theta 7$) do not change until the end of the test.

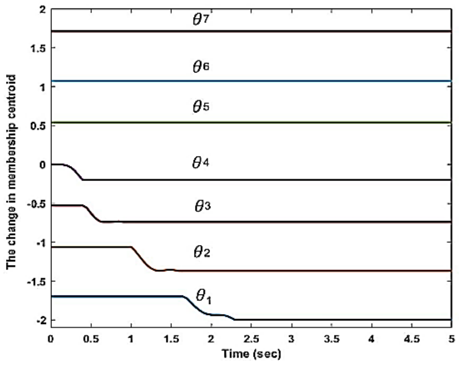

Figure 16. The change in membership centers during the variable position command test

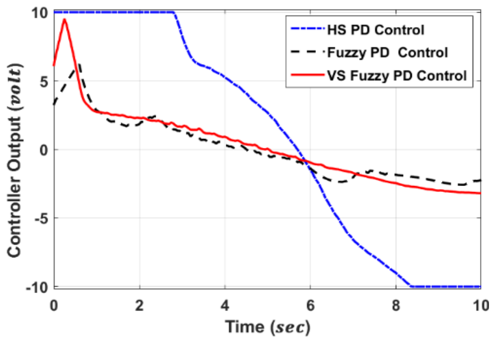

Figure 15. The control techniques output at variable position command

6. CONCLUSION

A new variable structure technique has been developed to tune the rule base of fuzzy logic control online based on optimal model reference adaptive system (MRAS). This work investigates the robustness of the proposed technique by applying it to one stage servomechanism system. The controller aims to track accurately a preselected position reference trajectory in presence of the friction and backlash problems. Also, the performance of the proposed controller technique has been compared to the classical PD control and the fixed structure fuzzy PD control to ensure robustness. There are two tests that have been implemented to investigate each control technique. The first test adjusts the position reference at a constant value while the second test adjusts the position reference to change continuously with time. The experimental results demonstrate that the variable structure fuzzy PD control based on an optimal model reference adaptive system can eliminate the tracking error quickly compared to other control techniques which will save the machining time cycles.

REFERENCES

[1] P. Zhao, J. Huang, and Y. Shi, "Nonlinear dynamics of the milling head drive mechanism in five-axis CNC machine tools," *International Journal Advanced Manufacturing Technology*, pp. 3195-3210, 2017, doi: 10.1007/s00170-017-9989-6.

[2] C. Abeykoon, "Single screw extrusion control: A comprehensive review and directions for improvements," *Control Engineering Practice*, vol. 51, pp. 69–80, 2016, doi: 10.1016/j.conengprac.2016.03.008.

[3] W. Lee, C. Lee, Y. H. Jeong, and B. Min, "Friction compensation controller for load varying machine tool feed drive," *International Journal of Machine Tools and Manufacture*, vol. 96, pp. 47–54, 2015, doi: 10.1016/j.ijmachtools.2015.06.001.

[4] C. Wang, M. Yang, W. Zheng, X. L.V., K. Hu and D. Xu, "Analysis of limit cycle mechanism for two-mass system with backlash nonlinearity," *Annual Conference of the IEEE Industrial Electronics Society*, 2016, pp. 500-505, doi: 10.1109/IECON.2016.7793734.

[5] F. Wang, C. Liang, Z. Ma, X. Zhao, Y. Tian and D. Zhang, "Dynamic analysis of an XY positioning table," in *International Conference on Manipulation, Manufacturing and Measurement on the Nanoscale*, 2013, pp. 211-214, doi: 10.1109/3M-NANO.2013.6737416.

[6] S. Yeh and J. Sun, "Feedforward motion control design for improving contouring accuracy of CNC machine tools," in *International Multi Conference of Engineers and Computer Scientists*, 2013.

[7] P. Zhao and Y. Shi, “Robust control of the A-axis with friction variation and parameters uncertainty in five-axis CNC machine tools,” *Journal of Mechanical Engineering Science*, 2014, doi: 10.1177/0954406213519759.
[8] B. Feng, D. Zhang, J. Yang, and S. Guo, “A novel time-varying friction compensation method for servomechanism,” *Hindawi: Mathematical Problems in Engineering*, pp. 1-16, 2015, doi: 10.1155/2015/269391.
[9] F. Wang, C. Liang, Y. Tian, X. Zhao and D. Zhang, “Design and control of a compliant microgripper with a large amplification ratio for high-speed micro manipulation,” in *IEEE/ASME Transactions on Mechatronics*, vol. 21, no. 3, pp. 1262-1271, 2016, doi: 10.1109/TMECH.2016.2523564.
[10] C. Liang, F. Wang, Y. Tian, X. Zhao, and D. Zhang, “Development of a high speed and precision wire clamp with both position and force regulations,” *Robotics and Computer-Integrated Manufacturing*, vol. 44, pp. 208–217, 2017, doi 10.1016/j.rcim.2016.09.006.
[11] F. Wang, X. Zhao, D. Zhang, Z. Ma, and X. Jing, “Robust and precision control for a directly-driven XY table,” *Journal of Mechanical Engineering Science*, vol. 225, pp. 1107–1120, 2011, doi: 10.1177/2041298310392832.
[12] F. Wang, Z. Ma, W. Gao, and X. Zhao, “Dynamic modeling and control of a novel XY positioning stage for semiconductor packaging,” *Transactions of the Institute of Measurement and Control*, vol. 37, no. 2, pp. 177–189, 2014, doi: 10.1177/0142331214541598.
[13] E. Yuliza, H. Habil, R. A. Salam, M. M. Munir, and M. Abdullah, Khairurrijal “Development of a simple single-axis motion table system for testing tilt sensors,” in *Engineering Physics International Conference (EPIC)*, 2017, vol. 170, pp. 378–383, doi: 10.1016/j.proeng.2017.03.061.
[14] P. Perz, I. Malujda, D. Wilczy, and P. Tarkowski, “Methods of controlling a hybrid positioning system using LabVIEW,” *International Polish-Slovak Conference: Machine Modeling and Simulations*, 2017, vol. 177, pp. 339–346, doi: 10.1016/j.proeng.2017.02.235.
[15] M. Chang and G. Guo, “Sinusoidal servocompensator implementations with real-time requirements and applications,” in *IEEE Transactions on Control Systems Technology*, vol. 25, no. 2, pp. 645-652, 2017, doi: 10.1109/TCST.2016.2558476.
[16] M. Irfan, M. Effendy, N. Alif, S. Lailis, I. Pakaya, and A. Faruq, “Performance comparison of fuzzy logic and proportional-integral for an electronic load controller,” *International Journal of Power Electronics and Drive System (IJPEDS)*, vol. 8, no. 3, pp. 1176–1183, 2017, doi: 10.11591/ijpeds.v8i3.pp1176-1183.
[17] M. A. Abdel Ghany, M. A. Shamseldin, and A. M. Abdel Ghany, “A novel fuzzy self tuning technique of single neuron PID controller for brushless DC motor,” *International Journal of Power Electronics and Drive System (IJPEDS)*, vol. 8, no. 4, pp. 1705-1713, 2017, doi: 10.11591/ijpeds.v8i4.pp1705-1713.
[18] U. K. Bansal and R. Narvey, “Speed control of DC motor using fuzzy PID controller,” *Advance in Electronic and Electric Engineering*, vol. 3, no. 9, pp. 1209–1220, 2013.
[19] I. Barkana, “Simple adaptive control-A stable direct model reference adaptive control methodology-brief survey,” *International Journal of Adaptive Control and Signal Processing*, vol. 28, no. 7–8, pp. 567–603, 2013, doi: 10.1002/acs.2411.
[20] T.H. Chiew, Z. Jamaludin, A.Y. Bani Hashim, L. Abdullah, N.A. Rafan and M. Maharof “Second order sliding mode control for direct drive positioning system,” *Journal of Mechanical Engineering and Sciences*, vol. 11, no. 4, pp. 3206–3216, 2017, doi: 10.15282/jmes.11.4.2017.23.0289.
[21] P. Jain, “Design of a model reference adaptive controller using modified MIT rule for a second order system,” *Advance in Electronic and Electric Engineering*, vol. 3, no. 4, pp. 477–484, 2013.
[22] N. Kumar, “Application of fractional order PID controller for AGC,” *International Journal of Automation and Computing*, vol. 15, pp. 84–93, 2018, doi: 10.1007/s11633-016-1036-9.
[23] S. Pankaj, J. S. Kumar, and R. K Nema, “Comparative analysis of MIT rule and lyapunov rule in model reference adaptive control scheme,” *Innovative Systems Design and Engineering*, vol. 2, no. 4, pp. 154–163, 2011.
[24] S. Y. Hwang, G. Y. Park, D. H. Kim, and K. S. Jhan, “Efficient implementation of a pseudorandom sequence generator for high-speed data communications,” *ETRI Journal*, vol. 32, no. 2, pp. 222–229, 2010, doi: 10.4218/etrij.10.1409.0047.
[25] B. J. Moore, T. Berger and D. Song, “Validation of a convolutional neural network model for spike transformation using a generalized linear model,” *Annual International Conference of the IEEE Engineering in Medicine & Biology Society (EMBC)*, 2020, pp. 3236-3239, doi: 10.1109/EMBC44109.2020.9176458.
[26] G. Sun, X. Ren and D. Li, “Neural active disturbance rejection output control of multimotor servomechanism,” *IEEE Transactions on Control Systems Technology*, vol. 23, no. 2, pp. 746-753, March 2015, doi: 10.1109/TCST.2014.2336595.
[27] B. Siegel, “Industrial anomaly detection: a comparison of unsupervised neural network architectures,” *IEEE Sensors Letters*, vol. 4, no. 8, pp. 1-4, Aug. 2020, Art no. 7501104, doi: 10.1109/LSENS.2020.3007880.
[28] Manuel Baltieri and Christopher L. Buckley, “PID control as a process of active inference with linear generative models,” *Entropy*, 2019, doi: 10.3390/e21030257.
[29] A. A. El-samahy and M. A. Shamseldin, “Brushless DC motor tracking control using self-tuning fuzzy PID control and model reference adaptive control,” *Ain Shams Engineering Journal*, 2016, doi: 10.1016/j.asej.2016.02.004.
[30] M. A. Shamseldin, M. A. Eissa, and A. A. El-samahy, “Practical implementation of GA-based PID controller for brushless DC motor,” *International Middle East Power System Conference (MEPCON'15)*, 2015.
[31] T. H Chiew, B. Hashim, A. Y, and N. A, Raffan “Identification of friction models for precise positioning system in machine tools,” *Procedia Engineering*, vol. 53, pp. 569–578, 2013, doi: 10.1016/j.proeng.2013.02.073.
[32] I. B. Tijani, R. Akmeliawati, A. Legowo, and A. Budiyono, “Nonlinear identification of a small scale unmanned helicopter using optimized NARX network with multiobjective differential evolution,” *Engineering Applications of Artificial Intelligence*, vol. 33, pp. 99–115, 2014, doi: 10.1016/j.engappai.2014.04.003.
[33] E. Cajueiro, R. Kalid and L. Schnitman, “Using NARX model with wavelet network to inferring the polished rod position,” *International Journal of Mathematics and Computers in Simulation*, vol. 6, no. 1, pp. 66-73, 2012.
[34] M. R. Stankovi, M. B. Naumović, S. M. Manojlović, and S. T. Mitrović, “Fuzzy model reference adaptive control of velocity servo system,” FACTA Universitas: Electronics Energetics, vol. 27, pp. 601–611, 2014, doi: 10.2298/FUEE1404601S.
[35] M. A. Shamseldin, A. A. EL-Samahy and A. M. A. Ghany, “Different techniques of self-tuning FOPID control for Brushless DC Motor,” *Eighteenth International Middle East Power Systems Conference (MEPCON)*, 2016, pp. 342-347, doi: 10.1109/MEPCON.2016.7836913.
[36] Vasadi Srinivasa Rao, P. D. Srinivas and Ch. Ravi Kumar “Load Frequency Control (LFC) of Three Area Interconnected Power System using Adaptive Neuro Fuzzy Interface System,” International Journal Scientific Engineering and Technology Research, vol. 4, no. 43, pp. 9482–9488, 2015.
[37] A. L. Elshafei, K. A. El-Metwally, and A. A. Shaltout, “A variable-structure adaptive fuzzy-logic stabilizer for single and multi-machine power systems,” *Control Engineering Practice*, vol. 13, no. 4, pp. 413–423, 2005, doi: 10.1016/j.conengprac.2004.03.017.

[38] P. Swarnkar, S. Jain, and R. K. Nema, "Effect of adaptation gain in model reference adaptive controlled second order system," *Engineering Technology and Applied Science Research*, vol. 1, no. 3, pp. 70–75, 2011, doi: 10.48084/etasr.11.

[39] M. Omar, M. A. Ebrahim, A. M, and F. Bendary, "Tuning of pid controller for load frequency control problem via harmony search algorithm," *Indonesian Journal of Electrical Engineering and Computer Science*, vol. 1, no. 2, pp. 255–263, 2016, doi: 10.11591/ijeecs.v1i2.pp255-263.

[40] M. Omar, A. M. A. Ghany, and F. Bendary, "Harmony search based PID for multi area load frequency control including boiler dynamics and nonlinearities," *WSEAS Transactions on Circuits and Systems*, vol. 14, pp. 407–414, 2015.

[41] M. A. Ebrahim and F. Bendary, "Reduced size harmony search algorithm for optimization," *Journal of Electricarl Engineering*, pp. 1–8, 2016.

BIOGRAPHIES OF AUTHORS

Mohamed A. Shamseldin received M.Sc. degree in system automation and engineering management and the Ph.D. degree in mechatronics engineering both from the Helwan University, Cairo, Egypt, in 2016 and 2020, respectively. In 2018, he was a Lecturer with the Faculty of Engineering, University of Central Lancashire, UK. Currently, he is an assistant Professor with the faculty of engineering and technology of Mechatronics Engineering, Future University in Egypt, Cairo, Egypt. His research interests include electric machine drives, mechatronics, robot control, system automation, and electric vehicle. He can be contacted at email: Mohamed.abelbbar@fue.edu.eg.

Abdel Halim M. Bassiuny was born in Egypt. He is professor at the department of mechanical engineering, faculty of engineering, Helwan University, Egypt. His research interests include fuzzy control, neuro-fuzzy, and adaptive control system theories and their applications, machine tool dynamics and control, condition monitoring and mechatronics. Dr.Bassiuny was granted a DAAD scholarship, during the interval 1986-1989, at the Group of Automatic Control and Technical Cybernetics, Wuppertal University, Germany. He can be contacted at email: abdelhalim.bassiuny@hu.edu.eg.

Abdel Ghany M. Abdel Ghany was born in Cairo. He received his B.Sc. and M.Sc. degrees in 1980 and 1987 from the Electrical Power System and Machines department, Helwan University, Cairo, Egypt. From 1989 to 1994, he got his Ph.D. in Computer Controlled Systems from the Institute of Control and Systems Engineering, Technical University of Wroclaw Poland. From 1994 to 1999, he worked as an assistant professor at the department of Electrical Machines and Power System, Helwan University, Cairo Egypt. In 2002, he was promoted to Professor at the Department of Electrical Power Systems and Machines Department, University of Helwan, Cairo, Egypt. Dr. Abdel Ghany shared in the Economical Lighting of Helwan industrial plant as a part of the Supreme Council of Egyptian Universities Projects. He can be contacted at email: Abdelghany.mohamed@thebes.edu.eg.